Electrochimica Acta 56 (2011) 4263–4267

Contents lists available at ScienceDirect

Electrochimica Acta

journal homepage: www.elsevier.com/locate/electacta

Synthesis of $LiFePO_4$/C cathode material from ferric oxide and organic lithium salts

Zhongqi Shi[a,b], Ming Huang[a,b], Yongjian Huai[a,b,c], Ziji Lin[a,b], Kerun Yang[a,b], Xuebu Hu[d,e], Zhenghua Deng[a,b,e,*]

[a] Chengdu Institute of Organic Chemistry, Chinese Academy of Sciences, Chengdu, Sichuan 610041, PR China
[b] Graduate School of Chinese Academy of Sciences, Beijing, 100039, PR China
[c] China Aviation Lithium Battery Co., Ltd, Luoyang, Henan 471003, PR China
[d] Department of Chemistry and Materials, Sichuan Normal University, Chengdu, Sichuan 610068, PR China
[e] Zhongke Laifang Power Science & Technology Co., Ltd., Chengdu, Sichuan 610041, PR China

ARTICLE INFO

Article history:
Received 30 October 2010
Received in revised form 17 January 2011
Accepted 22 January 2011
Available online 28 January 2011

Keywords:
Lithium iron phosphate
Organic lithium salt
Ferric oxide
Lithium-iron batteries

ABSTRACT

$LiFePO_4$/C cathode material has been simply synthesized via a modified in situ solid-state reaction route using the raw materials of Fe_2O_3, $NH_4H_2PO_4$, $Li_2C_2O_4$ and lithium polyacrylate (PAALi). The sintering temperature of $LiFePO_4$/C precursor is studied by thermo-gravimetric (TG)/differential thermal analysis (DTA). The physical properties of $LiFePO_4$/C are then investigated through analysis using by X-ray diffraction (XRD), scanning electron microscopy (SEM), transmission electron microscope (TEM) and the electrochemical properties are investigated by electrochemical impedance spectra (EIS), cyclic voltammogram (CV) and constant current charge/discharge test. The $LiFePO_4$/C composite with the particle size of ~200 nm shows better discharge capacity (156.4 mAh g^{-1}) than bare $LiFePO_4$ (52.3 mAh g^{-1}) at 0.2 C due to the improved electronic conductivity which is demonstrated by EIS. The as-prepared $LiFePO_4$/C through this method also shows excellent high-rate characteristic and cycle performance. The initial discharge capacity of the sample is 120.5 mAh g^{-1} and the capacity retention rate is 100.6% after 50 cycles at 5 C rate. The results prove that the using of organic lithium salts can obtain a high performance $LiFePO_4$/C composite.

1. Introduction

With a high voltage and energy density, lithium-ion batteries have become a new generation of green rechargeable batteries and have an increasingly diverse range of applications, from portable electronic devices to electric vehicle (EV) and hybrid electric vehicle (HEV). Widespread attentions have been paid upon the development of cathode material. Compared with $LiNiO_2$, $LiCoO_2$ and $LiMn_2O_4$, the most promising cathode material, olivine-type $LiFePO_4$ [1] presents several advantages, such as low material cost, no toxicity, high theoretical capacity (170 mAh g^{-1}), thermal stability at rather high temperature, safety and so on. However, $LiFePO_4$ suffers from two drawbacks of poor ionic conductivity and poor electronic conductivity, which are the major limitations of its large-scale application such as in electric vehicle. To overcome the problems, several methods have been developed, such as coating electronically conductive additives (carbon or metal) [2–5], doping with supervalent cation [6,7] and minimizing the particle size [8–10].

Currently, solid-state reaction [1,4,11] is considered as the appropriate method for commercial production of $LiFePO_4$. Meanwhile, Li_2CO_3 [1,5,12–14], LiOH H_2O [15–18] or CH_3COOLi [3,19,20] have been used frequently as the lithium source to synthesize $LiFePO_4$. It is well known that the divalent iron is stable in the acidic systems, but is inclined to be oxidized in the alkaline environment. The using of these lithium compounds in aqueous system will lead the precursor slurry to display alkalinity, which may impact the stability of the divalent iron. Moreover, the precursor may suffer from composition segregation which is caused by the fusion of these lithium compounds, because the fusion temperature of them is lower than the decomposition temperature. The segregation will gravely damage the homogeneity of the precursor, and then affect the performance of $LiFePO_4$.

From the above reviews, we use two organic lithium salts of $Li_2C_2O_4$ and lithium polyacrylate (PAALi) as the lithium source, Fe_2O_3 as the iron source and $NH_4H_2PO_4$ as the phosphorus source to synthesize carbon coated $LiFePO_4$ via solid-state reaction. Contracted with the method by using divalent iron compounds, only

* Corresponding author at: Chengdu Institute of Organic Chemistry, Chinese Academy of Sciences, Chengdu, Sichuan 610041, PR China. Tel.: +86 2885229252; fax: +86 2885233426.
E-mail address: zhdeng@cioc.ac.cn (Z. Deng).

0013-4686/$ – see front matter © 2011 Elsevier Ltd. All rights reserved.
doi:10.1016/j.electacta.2011.01.082

after reducing ferric iron to divalent iron can we obtain the $LiFePO_4$ when we use ferric oxide as iron source. As is well known, carboxylic acid free-radicals obtained from the pyrolysis of $Li_2C_2O_4$ have strong reducibilities, which can reduce ferric iron to divalent iron by a sequence of free-radical reactions [21–23]. PAALi can also generate carboxylic acid free radicals and is an effective dispersant in the mixture of starting materials. $Li_2C_2O_4$ and PAALi, which are different from inorganic lithium salts, can avoid the composition segregation and ensure the homogeneity of the precursor because the decompositions of the two organic lithium salts precede the fusions.

Meanwhile the aqueous PAALi is also used as carbon source. So we can use environmentally friendly and low cost distilled water as the dispersion medium, to replace the organic solvents, such as acetone and ethanol. Moreover, the using of ferric oxide can further reduce the production cost of $LiFePO_4$.

2. Experimental

Fe_2O_3, NH_4H_2 PO_4, $Li_2C_2O_4$, and PAALi were used as starting materials to synthesize $LiFePO_4$/C. PAALi was obtained via dissolving a stoichiometric amount of LiOH H_2O into an aqueous solution of polyacrylic acid (PAA). $Li_2C_2O_4$ and PAALi with an appropriate mixture mole ratio of 1.17:1, were used as lithium sources. Starting materials were placed in a stainless steel cylindrical container with zirconia ball and grounded in a planetary ball-miller for 8 h in water at a rotation speed of 400 rpm. The above mixture was dried in an oven at 100 °C for 10 h to get precursor and then preheated at 450 °C for 2 h and held at 700 °C for 10 h in an N_2 atmosphere. Bare $LiFePO_4$ was prepared without using PAALi.

TG–DTA measurements have been performed (NETZSCH STA 409 PC/PG) from 20 to 800 °C at a heating rate of 10 °C min^{-1} under argon atmosphere. The crystalline phase of the sample was identified by XRD analysis using Cu Kα radiation (X'Pert Pro MPD, PHILIP). The morphology of powder was observed by scanning electronic microscope (SEM, INSPECT F, FEI) and transmission electron microscope (TEM, JEM-100C, JEOL). The carbon content of samples was determined by an elemental analyzer (CARLO ERBA 1106, CARLO ERBA).

The cathodes were prepared via mixing 90 wt.% $LiFePO_4$/C composite, 5 wt.% conductive carbon black (Super P, TIMCAL) and 5 wt.% an aqueous binder LA132 (from Indigo, China) in distilled water. The resultant slurry was then coated onto an aluminum foil. The coated aluminum foil was dried for 10 h in a vacuum oven at 100 °C and then punched into circular discs with active material loading of about 4–5 mg cm^{-2}.

The lithium foil was used as the counter electrode and 1 M $LiPF_6$ in EC:DEC:EMC = 1:1:1 was used as the electrolyte. The 2032 type coin cells were assembled in an argon-filled glove box. The charged/discharged test was performed at various C rates in the voltage range of 2.5–4.3 V (versus Li/Li^+) at ambient temperature. Electrochemical impedance spectra (EIS) were investigated by a Solartron SI 1260/1287 (UK) impedance analyzer in the frequency range of 10^{-1}–10^6 Hz. Cyclic voltammetry (CV) tests were carried out in the voltage range of 2.5–4.3 V at a scan rate of 0.1 mV s^{-1} (Arbin-001 MITS Pro 3.0-BT2000, Arbin). All the tests were carried out at room temperature.

3. Results and discussion

Fig. 1 shows the TG/DTA curves for the precursor of $LiFePO_4$/C from 20 to 800 °C with a heating rate of 10 °C min^{-1} in an argon flow rate of 30 mL min^{-1}. The mass-loss process in the TG curve is related to exothermic and endothermic peaks in the DTA curve. An initial mass loss of 2.84% before 160 °C and an endothermic peak

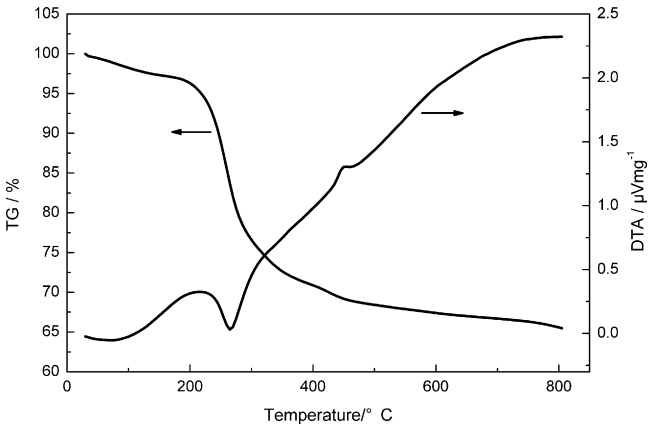

Fig. 1. TG–DTA curves of the $LiFePO_4$/C precursor recorded from 20 to 800 °C with a heating rate of 10 °C min^{-1} under an argon flow of 30 mL min^{-1}.

was observed. This is attributed to the volatilization of moisture of the precursor. A continuous mass loss between 200 and 450 °C can be related to the thermal decomposition of the partial reactants. There is a solely petite exothermic peak at 452.2 °C in the DTA curve, but no appreciable mass loss is observed in TG curve, this is suggesting that the crystallization of $LiFePO_4$ takes place in this temperature [24–26]. The mass of the precursor is almost unchanged after 600 °C, which may indicate that the reaction was complete. In this study, the precursor was preheated at 450 °C and finally held at 700 °C to get the well-crystallized $LiFePO_4$.

Fig. 2 shows the X-ray diffraction patterns for the bare $LiFePO_4$ and the $LiFePO_4$/C composite. All the two patterns can demonstrate a well-ordered olivine $LiFePO_4$, indexing to be an orthorhombic *Pmnb*, in good agreement with the JCPDS No. 83-2092. It indicates that $LiFePO_4$ can also be obtained from Fe_2O_3 by the reducibility of carboxylic acid free radicals, without adding carbon source PAALi. However, a petite Fe_2O_3 peak was detected in the bare $LiFePO_4$, whereas no impurities were observed in the $LiFePO_4$/C composite. The result means that reduction of Fe_2O_3 is not thorough only using $Li_2C_2O_4$ as reducing agent, but the problem is dissolved by the cooperation of $Li_2C_2O_4$ and PAALi. Meanwhile, no characteristic diffraction peaks of crystallized carbon was detected in the XRD pattern for $LiFePO_4$/C composite, it suggests that the presence of carbon delivered from PAALi does not influence the structure of $LiFePO_4$.

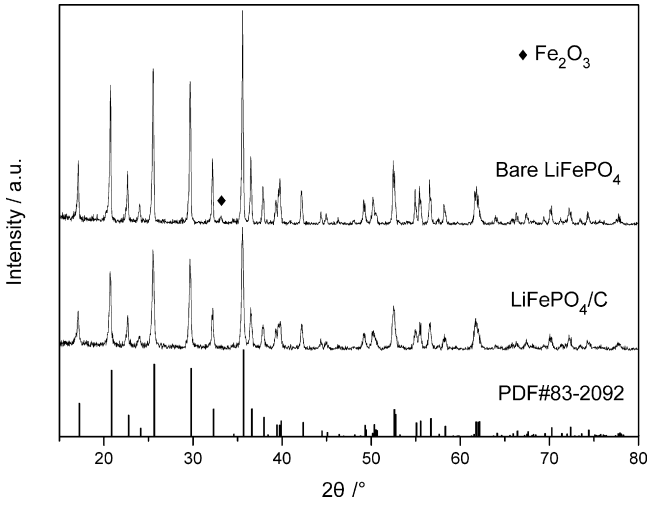

Fig. 2. XRD pattern of the $LiFePO_4$/C composite.

Table 1
The lattice parameters and calculated crystallite size (D) based on the (3 1 1) diffraction peaks for the pure $LiFePO_4$ and $LiFePO_4$/C composite.

Sample	a (Å)	b (Å)	c (Å)	V (Å^3)	D_{311} (nm)
$LiFePO_4$	10.34484	6.01641	4.70195	292.64	55
$LiFePO_4$/C	10.34979	6.01199	4.70267	292.61	38

The lattice parameters and the calculated crystallite size based on the (3 1 1) diffraction peaks for two samples are listed in Table 1. The crystallite size was calculated based on the Scherer formula: $D = k\lambda/\beta\cos\theta$, where k is 0.9, λ is 0.15406 nm and β is the full-width-at-half-maximum (FWHM) of the diffraction peak on a 2θ scale, respectively. It can be observed that the lattice parameters of two samples have almost the same values, which are well accordant with the standard lattice parameter (a = 10.3344 Å, b = 6.0083 Å, c = 4.693 Å). However, the D_{311} are 55 nm for pure $LiFePO_4$ and 38 nm for $LiFePO_4$/C composite. It is believed that crystallite size may be reduced with the presence of the carbon.

Fig. 3 shows the SEM image of the $LiFePO_4$/C particles. Spherical-like particles are obtained and the average particle size remains in the range of 100–300 nm, which is contribute to improve the electrochemical properties of the sample. In order to determine the particle size and the carbon morphology, TEM was used. Fig. 4 shows that the $LiFePO_4$ particles have sphere-like shape, with the size ranging from 100 to 300 nm. It is obvious that the carbon webs formed from the decomposition of PAALi are wrapping and connecting the $LiFePO_4$ particles. The presence of carbon webs plays an important role in inhibiting the growth of $LiFePO_4$ particles and improving the electronic conductivities of materials. $LiFePO_4$/C composite contains 3.76 wt.% of carbon as determined by the elemental analyzer.

Fig. 5 presents the Nyquist plots of bare $LiFePO_4$ and $LiFePO_4$/C composite cathode. All the spectra have a semicircle and a linear spike in the high-frequency and low-frequency regions. The semicircle refers to the charge-transfer resistance of electrochemical reaction and the linear spike refers to the thin-layer ionic diffusion-controlled Warburg impedance [27–29]. Significant decrease of impendence from bare $LiFePO_4$ to $LiFePO_4$/C is related to the improved conductivity. According to the formula $\sigma = d/AR$ [30], the conductivities of $LiFePO_4$/C and bare $LiFePO_4$ are 4.4×10^{-6} and 2.1×10^{-6} S cm^{-1}, respectively. The increase conductivity is mainly due to the enhanced electronic conductivity because of the presence of the pyrolytic carbon webs.

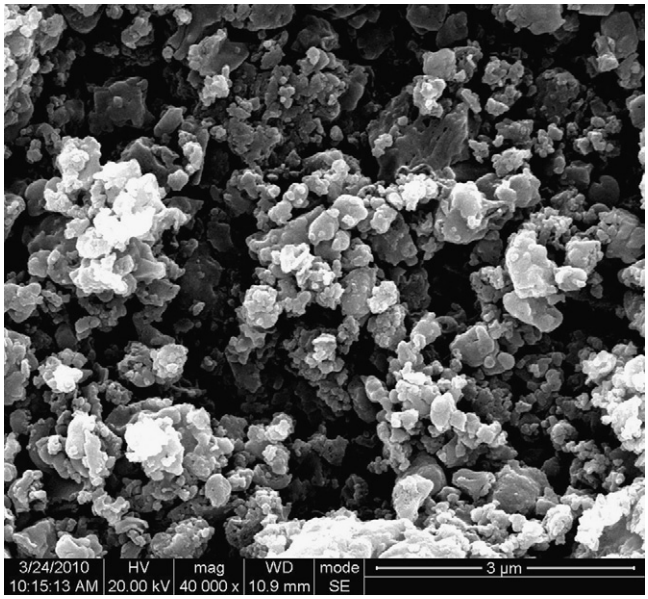

Fig. 3. SEM image of the $LiFePO_4$/C composite.

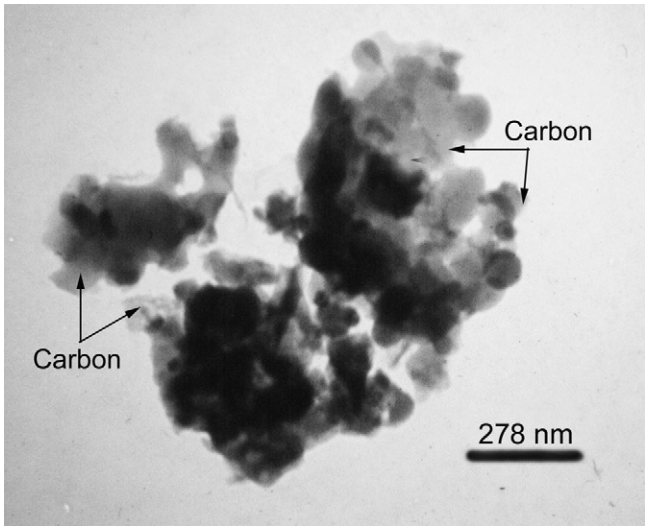

Fig. 4. TEM image of the $LiFePO_4$/C composite.

The initial charge–discharge curves of the obtained bare $LiFePO_4$ and $LiFePO_4$/C composite at 700 °C are shown in Fig. 6. When the cell was cycled between 2.5 and 4.3 V at 0.2 C-rate, the potential difference between charge and discharge plateau of $LiFePO_4$/C is 60 mV, which is much smaller than that of bare $LiFePO_4$. It indicates that the $LiFePO_4$/C exhibits much smaller polarization, which is mainly attributed to the improved conductivity by coated-carbon. The bare $LiFePO_4$ shows an initial discharge capacity of only 52.3 mAh g^{-1}, while the $LiFePO_4$/C shows a much higher initial discharge capacity of 156.4 mAh g^{-1} corresponding to 92% of the theoretical capacity. The growth of the discharge capacity is also ascribed to the presence of carbon webs improving the conductivity.

Fig. 7 shows the CV profiles of the $LiFePO_4$/C sample. In each cycle, we can only find one anodic peak and one cathodic peak, which correspond to the two-phase charge/discharge reaction of the Fe^{2+}/Fe^{3+} redox couple. The good overlap of the peaks indicates the good reversibility of the composite cathode, the small voltage interval between the anodic and cathodic peaks and high peak currents indicate the small electrode polarization once again.

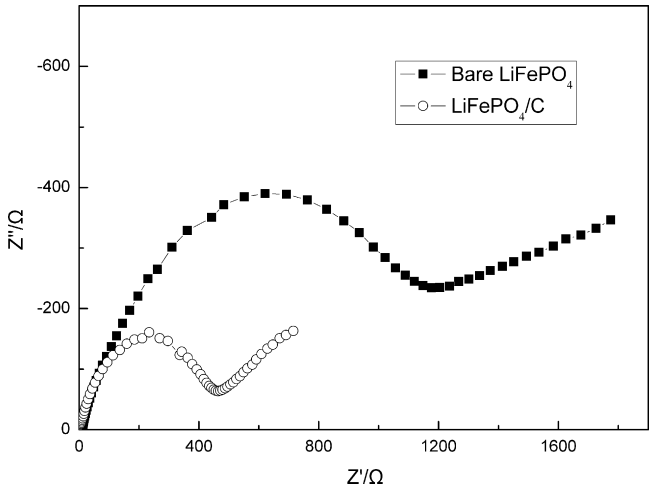

Fig. 5. Nyquist plots of bare $LiFePO_4$ and $LiFePO_4$/C composite with the frequency range of 10^{-1}–10^6 Hz.

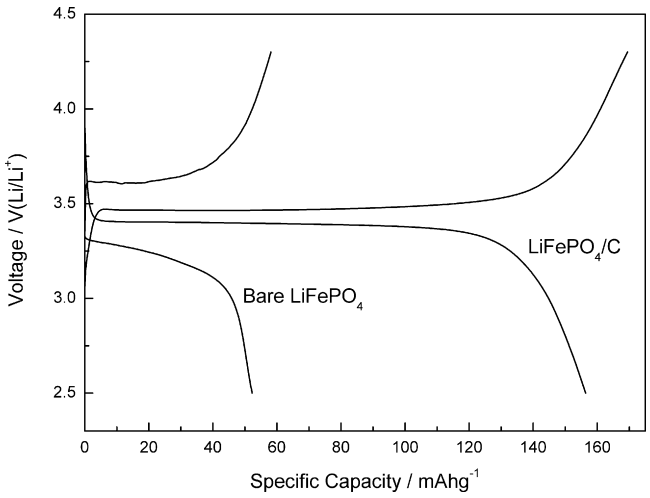

Fig. 6. Initial charge–discharge curves of the bare $LiFePO_4$ and the $LiFePO_4$/C composite at 0.2 C between 2.5 and 4.3 V.

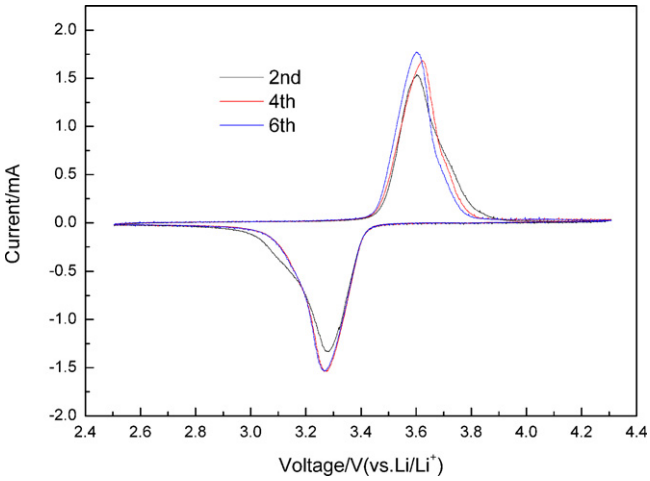

Fig. 7. CV profiles of the $LiFePO_4$/C sample in the voltage range of 2.5–4.3 V at a scan rate of 0.1 mV s^{-1}.

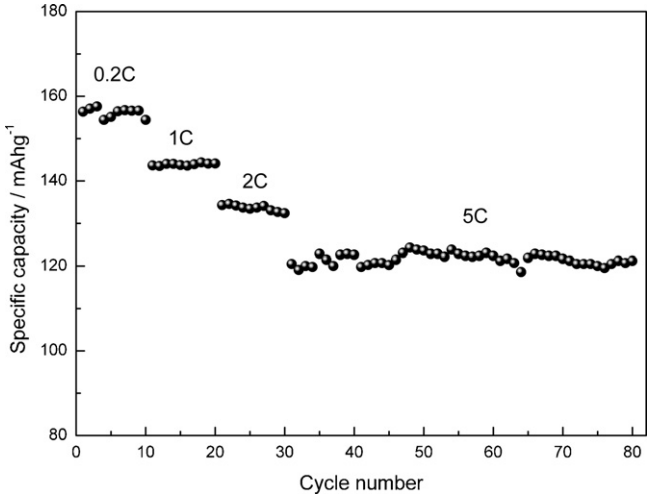

Fig. 8. Cycle performance of the $LiFePO_4$/C composite at different rates.

The $LiFePO_4$/C sample also shows good cycling performance at rates varying from 0.2 to 5 C-rate, as shown in Fig. 8. We can obtain a high specific capacity of 156.4 mAh g^{-1} in the initial discharge at 0.2 C and stable capacity without fading. With increasing the discharge rates, the discharge capacity decrease. Even at high rates at 5 C, it still remains high discharge capacities of 120.5 mAh g^{-1}. After 50 cycles, it presents the discharge capacities of 121.2 mAh g^{-1}, and exhibits excellent cycle retention. Meanwhile the increased capacity is probably due to the formation of fissures [12]. In comparison to several papers for carbon coated $LiFePO_4$ by other groups, such as Zhang et al. [18], Liu et al. [31] and Zhang et al. [32], $LiFePO_4$/C composite synthesized through our method exhibits higher discharge capacity at high rate and better cycling performance. Thus, the pyrolytic carbon delivered from PAALi improved the electrochemical performance, especially the cycling stability. Further studies are in progress.

4. Conclusions

In this work, we proved that well-ordered olivine $LiFePO_4$ can be synthesized with the carboxylic acid free radicals from $Li_2C_2O_4$ as reducing agent, and pure olivine-type $LiFePO_4$/C was successfully synthesized by this method, using $Li_2C_2O_4$ and PAALi as lithium source. The main advantage of this method is that our raw materials will not lead to the composition segregation during the sintering process. The $LiFePO_4$/C composite shows higher specific capacity and smaller polarization than the bare $LiFePO_4$. The initial discharge capacity of the $LiFePO_4$/C sample was 156.4 and 120.5 mAh g^{-1} at 0.2 C and 5 C rate, respectively. The excellent performance is probably due to the high electronic conductivity which is improved by the carbon web, produced in situ by the calcination of PAALi. Moreover, all the raw materials of this method are environment friendly and low cost, so it is suitable for commercial production of $LiFePO_4$ cathode material.

References

[1] A.K. Padhi, K.S. Nanjundaswamy, J.B. Goodenough, J. Electrochem. Soc. 144 (1997) 1188.
[2] N. Ravet, Y. Chouinard, J.F. Magnan, S. Besner, M. Gauthier, M. Armand, J. Power Sources 97–8 (2001) 503.
[3] M.S. Bhuvaneswari, N.N. Bramnik, D. Ensling, H. Ehrenberg, W. Jaegermann, J. Power Sources 180 (2008) 553.
[4] C.H. Mi, G.S. Cao, X.B. Zhao, Low-cost, Mater. Lett. 59 (2005) 127.
[5] H.C. Shin, S.B. Park, H. Jang, K.Y. Chung, W.I. Cho, C.S. Kim, B.W. Cho, Electrochim. Acta 53 (2008) 7946.
[6] S.Y. Chung, J.T. Bloking, Y.M. Chiang, Nat. Mater. 1 (2002) 123.
[7] M.S. Islam, D.J. Driscoll, C.A.J. Fisher, P.R. Slater, Chem. Mater. 17 (2005) 5085.
[8] A. Yamada, S.C. Chung, K. Hinokuma, J. Electrochem. Soc. 148 (2001) A224.
[9] C. Delacourt, P. Poizot, S. Levasseur, C. Masquelier, Electrochem. Solid State Lett. 9 (2006) A352.
[10] C.R. Sides, F. Croce, V.Y. Young, C.R. Martin, B. Scrosati, Electrochem. Solid State Lett. 8 (2005) A484.
[11] H.S. Kim, B.W. Cho, W.I. Cho, J. Power Sources 132 (2004) 235.
[12] J.K. Kim, J.W. Choi, G.S. Chauhan, J.H. Ahn, G.C. Hwang, J.B. Choi, H.J. Ahn, Electrochim. Acta 53 (2008) 8258.
[13] H.P. Liu, Z.X. Wang, X.H. Li, H.J. Guo, W.J. Peng, Y.H. Zhang, Q.Y. Hu, J. Power Sources 184 (2008) 469.
[14] X. Xia, Z.X. Wang, L.Q. Chen, Electrochem. Commun. 10 (2008) 1442.
[15] C.W. Kim, J.S. Park, K.S. Lee, J. Power Sources 163 (2006) 144.
[16] A. Kuwahara, S. Suzuki, M. Miyayama, Ceram. Int. 34 (2008) 863.
[17] H.W. Liu, H.M. Yang, J.L. Li, Electrochim. Acta 55 (2010) 1626.
[18] W.K. Zhang, X.Z. Zhou, X.Y. Tao, H. Huang, Y.P. Gan, C.T. Wang, Electrochim. Acta 55 (2010) 2592.
[19] H.W. Liu, D.G. Tang, Solid State Ionics 179 (2008) 1897.
[20] A. Fedorková, A. Nacher-Alejos, P. Gómez-Romero, R. Orináková, D. Kaniansky, Electrochim. Acta 55 (2010) 943.
[21] M. Kimura, I.M. Kolthoff, E.J. Meehan, J. Phys. Chem. 77 (1973) 1262.
[22] B.A. DeGraff, G.D. Cooper, J. Phys. Chem. 75 (1971) 2897.
[23] G. Kornfeld, J. Phys. Chem. 44 (1940) 949.
[24] P.P. Prosini, M. Carewska, S. Scaccia, P. Wisniewski, S. Passerini, M. Pasquali, J. Electrochem. Soc. 149 (2002) A886.
[25] F. Yu, J.J. Zhang, Y.F. Yang, G.Z. Song, Electrochim. Acta 54 (2009) 7389.

[26] Y.Q. Wang, J.L. Wang, J. Yang, Y.N. Nuli, Adv. Funct. Mater. 16 (2006) 2135.
[27] S. Rodrigues, N. Munichandraiah, A.K. Shukla, J. Solid State Electrochem. 3 (1999) 397.
[28] F. Nobili, F. Croce, B. Scrosati, R. Marassi, Chem. Mater. 13 (2001) 1642.
[29] M.D. Levi, D. Aurbach, J. Phys. Chem. B 101 (1997) 4630.
[30] Z.J. Lin, X.B. Hu, Y.J. Huai, L. Liu, Z.H. Deng, J.S. Suo, Solid State Ionics 181 (2010) 412.
[31] Y.Y. Liu, C.B. Cao, J. Li, Electrochim. Acta 55 (2010) 3921.
[32] Y. Zhang, H. Feng, X.B. Wu, L.Z. Wang, A.Q. Zhang, T.C. Xia, H.C. Dong, M.H. Liu, Electrochim. Acta 54 (2009) 3206.